Stereoselectivity of a Potent Calcium Antagonist, 1-Benzyl-3-pyrrolidinyl Methyl 2,6-Dimethyl-4-(m-nitrophenyl)-1,4-dihydropyridine-3,5-dicarboxylate

Kazuharu Tamazawa,* Hideki Arima, Tadao Kojima, Yasuo Isomura, Minoru Okada, Shigeo Fujita, Toshio Furuya, Toichi Takenaka, Osamu Inagaki, and Michio Terai

Central Research Laboratories, Yamanouchi Pharmaceutical Company, Ltd., No. 1-8, Azusawa-1-Chome, Itabashi-Ku, Tokyo 174, Japan. Received December 30, 1985

Four enantiomers (3a–d) of the title compound, YM-09730 (3), were synthesized by the reaction of (-)- or (+)-5-(methoxycarbonyl)-2,6-dimethyl-4-(m-nitrophenyl)-1,4-dihydropyridine-3-carboxylic acid (1a or 1b) with (S)- or (R)-1-benzyl-3-pyrrolidinol (2a or 2b). [^{3}H]Nitrendipine binding affinity and coronary vasodilating activity of these compounds were evaluated. The absolute configuration of the most potent enantiomer (3a) with the longest duration was unequivocally determined to be (S)-1,4-dihydropyridine-C4 and (S)-pyrrolidine-C3 (S,S) by X-ray crystallographic study on 3a·HBr as well as 3a·HCl. The configuration of 1a corresponds to R, and the other enantiomers of 3 were respectively determined by chemical correlation. The potency order of the four enantiomers was (S,S)-3a > (S,R)-3b > (R,R)-3d > (R,S)-3c. Latent chiral characters of nifedipine derivatives with the identical ester groups were assigned by comparison of their puckering modes of 1,4-dihydropyridine (DHP) rings with those found in 3a·HCl or 3a·HBr. On the basis of the assignment, it has been revealed that the (S)-DHP nifedipine derivatives possess the synperiplanar carbonyl group at C5. The conformational restriction may be a factor causing stereoselectivity of antagonism.

1,4-Dihydropyridine (DHP) derivatives constitute a major class of calcium antagonists and have been a target of structure–activity relationship studies. Some remarkable findings were reviewed by Janis and Triggle.[1] Stereoselectivity of calcium antagonism has been observed in many DHP compounds whose ester substituents at C3 and C5 positions are different,[2-8] but it was merely suggested that the binding of those compounds occurred at a stereoselective site of receptor. Recently, several crystallographic studies have correlated the pharmacological effects with the degree of puckering of DHP rings.[9] The more active compounds exhibit the smaller degree of distortion from planarity, but the mechanism of stereoselectivity still remains uncertain. Configurational and conformational factors contributing to the stereoselectivity are interesting.

The title compound (YM-09730, 3), with two chiral centers, has been previously found to be very potent in producing marked hypotension of long duration when administered orally to spontaneously hypertensive rats.[10] We have successfully prepared each enantiomer (3a–d), evaluated its activity,[11] and determined the absolute configuration of the most potent enantiomer (3a) by X-ray crystallography. As a part of the study of stereochemical

Table I. Inhibition of [^{3}H]Nitrendipine Binding to Rat Brain Cortex Homogenate Membranes

drug	K_i[a] nmol L	Hill coefficient
3a·HCl (S,S)	0.205 (0.17–0.25)	1.203
3b·HCl (S,R)	3.09 (2.14–4.44)	0.752
3c·HCl (R,S)	49.6 (39.1–62.9)	0.957
3d·HCl (R,R)	14.3 (10.2–20.1)	1.143
(+)-nicardipine (S)	0.499 (0.43–0.58)	1.286
(-)-nicardipine (R)	7.11 (5.43–9.31)	1.241
(±)-nitrendipine	0.840 (0.73–0.96)	1.054
nifedipine	4.65 (4.16–5.20)	1.105

[a] Figures in parentheses show 95% confidence limits.

structure–activity relationships, correlation between chirality of the DHP ring and conformation of the carbonyl groups is discussed on the basis of the three-dimensional structures of DHP compounds.
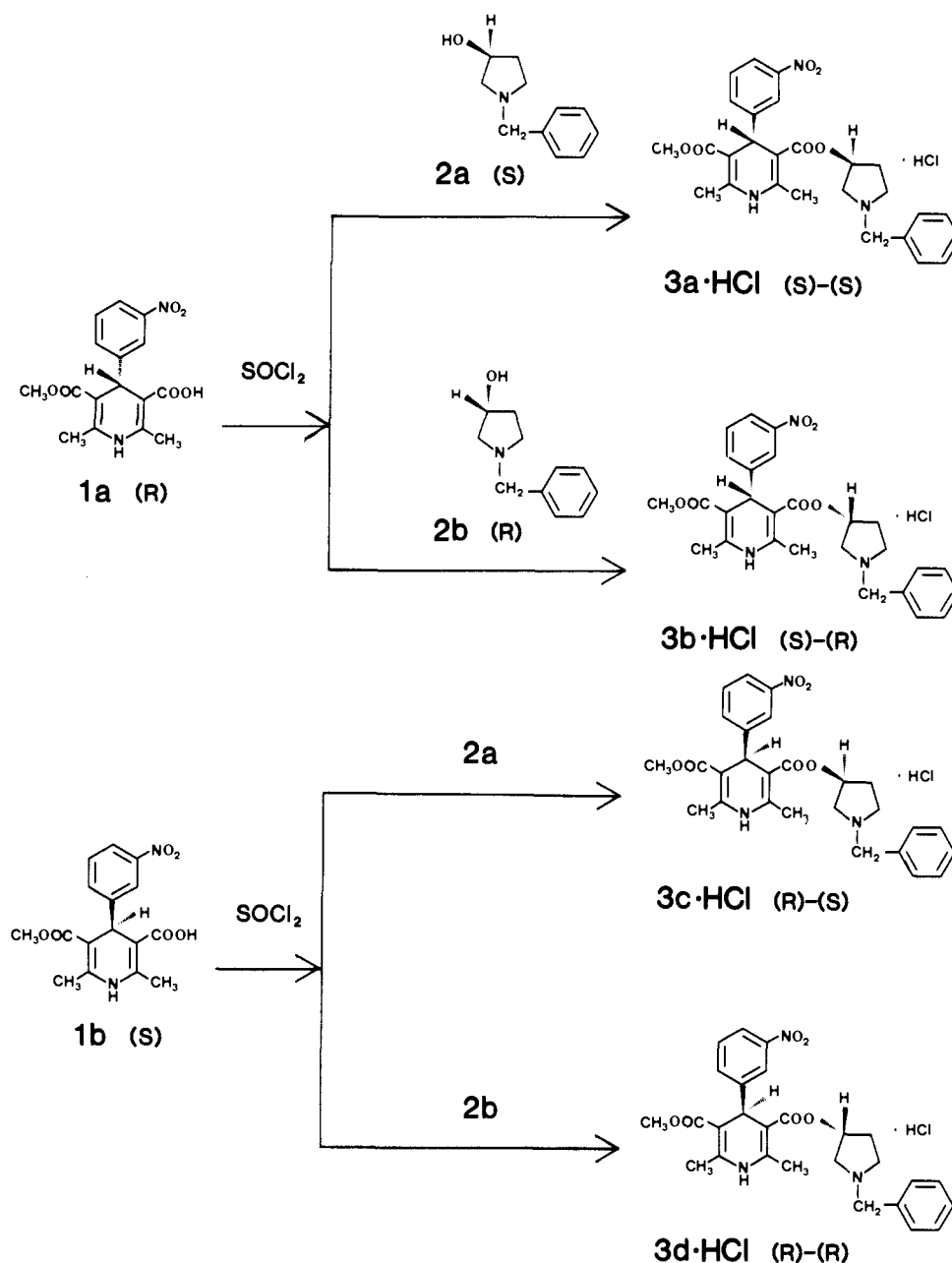
Chemistry

Levorotatory half-ester 1a, (-)-5-(methoxycarbonyl)-2,6-dimethyl-4-(m-nitrophenyl)-1,4-dihydropyridine-3-carboxylic acid, and its enantiomer 1b were synthesized by the method of Shibanuma et al.[2] Optically pure alcohols 2a and 2b were obtained via resolution of racemic 1-benzyl-3-pyrrolidinol (2)[12] with use of (R)-mandelic acid. The S-enantiomer 2a was also prepared by NaBH$_4$–BF$_3$ reduction of (S)-1-benzyl-3-hydroxysuccinimide, which was obtained by the reaction of (S)-malic acid and benzylamine.[13] Half-ester 1a was treated with thionyl chloride followed by the reaction with 2a to yield (+)-3a·HCl. Similarly, (+)-3b·HCl, (-)-3c·HCl, and (-)-3d·HCl were yielded (Scheme I). The absolute configuration of 3a was determined to be S,S[14] by X-ray crystallography (Figure 1). Therefore, the configuration of half-ester 1a corresponds to R and that of its enantiomer 1b is S.[15] Absolute

(1) Janis, R. A.; Triggle, D. J. *J. Med. Chem.* **1983**, *26*, 775.
(2) Shibanuma, T.; Iwanami, M.; Okuda, H.; Takenaka, T.; Murakami, M. *Chem. Pharm. Bull.* **1980**, *28*, 2809.
(3) Takenaka, T.; Miyazaki, I.; Asano, M.; Higuchi, S.; Maeno, H. *Jpn. J. Pharmacol.* **1982**, *32*, 665.
(4) Rosengerger, L. B.; Ticku, M. K.; Triggle, D. J. *Can. J. Physiol. Pharmacol.* **1979**, *57*, 333.
(5) Bossert, F.; Meyer, H.; Wehinger, F. *Angew. Chem., Int. Ed. Engl.* **1981**, *20*, 762.
(6) Mayer, H.; Bossert, F.; Wehinger, E.; Stoepel, K.; Vater, W. *Arzneim.-Forsch.* **1981**, *31*, 407.
(7) Towart, R.; Wehinger, E.; Meyer, H. *Naunyn-Schmiedeberg's Arch. Pharmacol.* **1981**, *317*, 183.
(8) Towart, R.; Wehinger, E.; Meyer, H.; Kazda, S. *Arzneim.-Forsch.* **1982**, *32*, 338.
(9) (a) Triggle, A. M.; Shefter, E.; Triggle, D. J. *J. Med. Chem.* **1980**, *23*, 1442. (b) Fossheim, R.; Svarteng, K.; Mostad, A.; Romming, C.; Shefter, E.; Triggle, D. J. *J. Med. Chem.* **1982**, *25*, 126.
(10) Kojima, T.; Takenaka, T. U.S. Patent 4 220 649, Jan. 31, 1979. See also: Prous, J.; Blancafort, P.; Castaner, J.; Serrandell, M. N.; Mealy, N. *Drugs of the Future* **1981**, *6*, 431; J. R. Prous, S. A. Publishers: Barcelona, Spain.
(11) Takenaka, T.; Inagaki, O.; Terai, M.; Kojima, T.; Tamazawa, K.; Arima, H.; Isomura, Y.: (a) 58th General Meeting of the Japanese Pharmacological Society, Tokyo, March 29, 1985; O4G1000. (b) *Jpn. J. Pharmacol.* **1985**, *39*, 215P.

(12) Lunsford, C. D.; Ward, J. W.; Pallotta, A. J.; Tusing, T. W.; Rose, E. K.; Murphey, R. S. *J. Med. Pharm. Chem.* **1959**, *1*, 73.
(13) Synthesis of 2a with 84% of enantiomeric purity was reported. Bhat, K. L.; Flanagan, D. M.; Joullie, M. M. *Synth. Commun.* **1985**, *15*, 587.
(14) The first and second symbols in parentheses indicate the configurations of the 1,4-dihydropyridine C4 position and the pyrrolidine C3 position, respectively.
(15) (+)-Nicardipine obtained from 1a is, therefore, correlated to be S. S configuration of (-)-isopropyl methyl 2,6-dimethyl-4-(m-nitrophenyl)-1,4-dihydropyridine-3,5-dicarboxylate (Towart et al., ref 7) was confirmed: (-)-(S)-isopropyl ester of 1a was obtained by the reaction of acid chloride of 1a with 2-propanol ([α]$^{20}_D$ -21.3° (c 1, ethanol).

Figure 1. Structure of **3a**·HCl (above) and **3a**·HBr (below) with atomic numbering. The torsion angles of ϕ[C2–C3–C31–O32], ϕ[C6–C5–C51–O52], ϕ[C3–C4–C7–C8], and ϕ[C3–C4–C7–C12] of **3a**·HCl are −4(2), −11(3), 51(2), and −130(2)°, and those of **3a**·HBr are 176.5(7), 4(1), 88(1), and −90.3(7), respectively.

configurations of the other enantiomers were chemically correlated as follows: **3b** (S,R), **3c** (R,S), and **3d** (R,R).

Then we focused our efforts on the practical synthesis of **3a**, which was found to be the most potent enantiomer. By fractional crystallization of acid salts of modified Hantzsch reaction products, **3a** was successfully isolated. Hantzsch reaction product **3**[10] in Scheme II was a mixture of two pairs of enantiomers, (±)-diastereomer A (**3e**) and (±)-diastereomer B (**3f**). Reversed-phase ion-pair high-performance liquid chromatography (HPLC) showed two main peaks with approximately equal areas. The peaks with shorter and longer retention time correspond to **3e** and **3f**, respectively. Treatment of **3** with malonic acid gave crystals of **3e** malonate. Subsequently, **3a** was obtained by optical resolution of **3e** with use of (S)-malic acid. As shown in Scheme III, the (S)-malic acid salt of **3a** was also separated from Hantzsch reaction product **3g**, diastereomeric mixture of **3a** and **3c** (ca. 1:1 by HPLC). The crude product was purified in the form of crystalline **3g** oxalate and converted to free base **3g**. With use of (S)-malic acid, **3a** (S)-malate was preferentially crystallized in good yield. The latter method is practical for large-scale synthesis of **3a** from the viewpoint of overall yield.

Pharmacology

[3H]Nitrendipine has been employed to directly identify putative Ca^{2+} channels in various tissue membranes.[16–21]

Figure 2. Effects of four enantiomers of **3** on coronary blood flow in anesthetized dogs after each 1 μg directly injected into the coronary artery. The abscissa indicates percent of increase in coronary blood flow, and the ordinate indicates time (minutes) after the injection. **3a** (■), **3b** (●), **3c** (X), and **3d** (△) were used. Each point is the mean of five experiments.

Table II. Comparative Vasodilator Activity

drug	ED_{100}, μg ia	AUC at 1 μg ia,[a] % min
3a·HCl	0.57	6155 ± 898 (0–120)
3b·HCl	1.6	300 ± 36 (0–15)
3c·HCl	9.1	31 ± 6 (0–2)
3d·HCl	3.1	73 ± 13 (0–5)

[a] Figures in parentheses show the duration (minutes).

Effects of each of four enantiomers of **3** on [3H]nitrendipine binding were determined. Each enantiomer was able to displace more than 85% of [3H]nitrendipine bound specifically. Individual K_i values were calculated and are summarized in Table I.[22] The potency order was **3a**·HCl > **3b**·HCl > **3d**·HCl > **3c**·HCl. The affinity of **3a**·HCl with the S,S configuration to [3H]nitrendipine binding sites was 240 times larger than that of **3c**·HCl (R,S), and the affinity of **3b**·HCl (S,R) was 4.6 times greater than that of **3d**·HCl (R,R). The enantiomer **3a**·HCl (S,S) was about 15 times as potent as **3b**·HCl (S,R). On the other hand, the affinity of **3d**·HCl (R,R) was about 3.5 times greater than that of **3c**·HCl (R,S). These indicate that the S configuration at C4 of the DHP ring is preferred by Ca^{2+} channel binding sites and that the configuration at C3 of the pyrrolidine ring also influences the affinity of **3**, although less pronouncedly than at C4 of the DHP ring.

Coronary vasodilating activity of each enantiomer was also evaluated in anesthetized coronary perfused dogs. Changes in coronary blood flow after direct administration of 1 μg of **3** into the coronary artery are shown in Figure 2. Heart rate and systemic mean blood pressure were not influenced. The ED_{100} values (the doses required for 100% increase in coronary blood flow at the peak time) of four enantiomers are summarized in Table II. The potency order was consistent with that of the binding affinity. The duration of activity of **3a**·HCl was much longer than that of **3b**·HCl, **3c**·HCl, and **3d**·HCl. Coronary vasodilating activity estimated by the area under increased blood flow curve (AUC) of **3a**·HCl was respectively 21, 84, and 199

(16) Gould, R. J.; Murphy, K. M. M.; Snyder, S. H. *Proc. Natl. Acad. Sci. U.S.A.* **1982**, *79*, 3656.

(17) Bellemann, P.; Ferry, D.; Lubbecke, F.; Glossmann, H. *Arzneim.-Forsch.* **1981**, *31*, 2064.

(18) Glossmann, H.; Ferry, D. R.; Lubbecke, F.; Mewes, R.; Hofmann, F. *Trends Pharmacol. Sci.* **1982**, *3*, 431.

(19) Bolger, G. T.; Gengo, P.; Klockowski, R.; Luchowski, E.; Siegel, H.; Janis, R. A.; Triggle, A. M.; Triggle, D. J. *J. Pharmacol. Exp. Ther.* **1983**, *225*, 291.

(20) Bristow, M. R.; Ginsburg, R.; Laser, J. A.; McAuley, B. J.; Minobe, W. *Br. J. Pharmacol.* **1984**, *82*, 309.

(21) Thayer, S. A.; Welcome, M.; Chhabra, A.; Fairhurst, A. S. *Biochem. Pharmacol.* **1985**, *34*, 175.

(22) Compound **1a** was a weak inhibitor of [3H]nitrendipine binding with a K_i value of 1.5 μM and 12 times more potent than **1b**.

Scheme I

2a (S)

1a (R)

SOCl₂

2b (R)

3a·HCl (S)-(S)

3b·HCl (S)-(R)

1b (S)

SOCl₂

2a

2b

3c·HCl (R)-(S)

3d·HCl (R)-(R)

times more potent than that of 3b·HCl, 3d·HCl, and 3c·HCl (Figure 2, Table II). A good correlation was obtained between the coronary vasodilating activity and the K_i values. Thus, potent activity with long duration found in YM-09730[10] resides in 3a·HCl with S,S configuration. Compound 3a·HCl (YM-09730-5) is now in clinical trial.

X-ray Crystallography

Perspective drawings of 3a·HCl and 3a·HBr are shown in Figure 1. The orientations of the carbonyl groups at C3 and C5 of 3a·HCl are both synperiplanar (*sp*) to the C2–C3 double bond and the C5–C6 double bond, but those of 3a·HBr are antiperiplanar (*ap*) to the C2–C3 double bond and *sp* to the C5–C6 double bond. The conformations of the *m*-nitrophenyl ring relative to the DHP ring are also different. The nitro group of 3a·HCl is pointed away from the DHP ring, but that of 3a·HBr is pointed toward the DHP ring (see the legend of Figure 1). The torsion angles (τ) of the intra 1,4-dihydropyridine ring around the N1–C2, C2–C3, C3–C4, C4–C5, C5–C6, and C6–N1 bonds are −10(2), −8(2), 20(2), −20(2), 5(2), and 11(2)° in 3a·HCl and −19.0(9), −7.3(9), 30.2(8), −30.9(8),

8.9(9), and 18.0(9)° in 3a·HBr. In both 3a·HCl and 3a·HBr, the degree of the ring distortion is greatest at C4 and N1, and the boat-type conformation is formed with apexes at C4 and N1 and with priapic orientation of the nitrophenyl ring at C4. This characteristic feature is commonly observed with DHP derivatives in free form[9b] and is also associated with 3a·HCl and 3a·HBr.

Discussion

As described in the pharmacological section, the S-configuration preference at C4 of 3, with two chiral centers, was observed. Other DHP derivatives, such as nicardipine, with one chiral center, have also been reported to show S-configuration preference at C4.[2,7,8,15] Therefore, it may be concluded that the (4S)-DHP isomer is generally more potent than the (4R)-DHP isomer.

Next we discuss a structural factor causing stereoselective antagonism observed in chiral DHP derivatives. The characteristic conformation of the DHP ring and two types of carbonyl arrangements found in 3a·HCl (*sp,sp*) and 3a·HBr (*ap,sp*) are commonly observed in the molecular structures of calcium antagonists of nifedipine

Scheme II
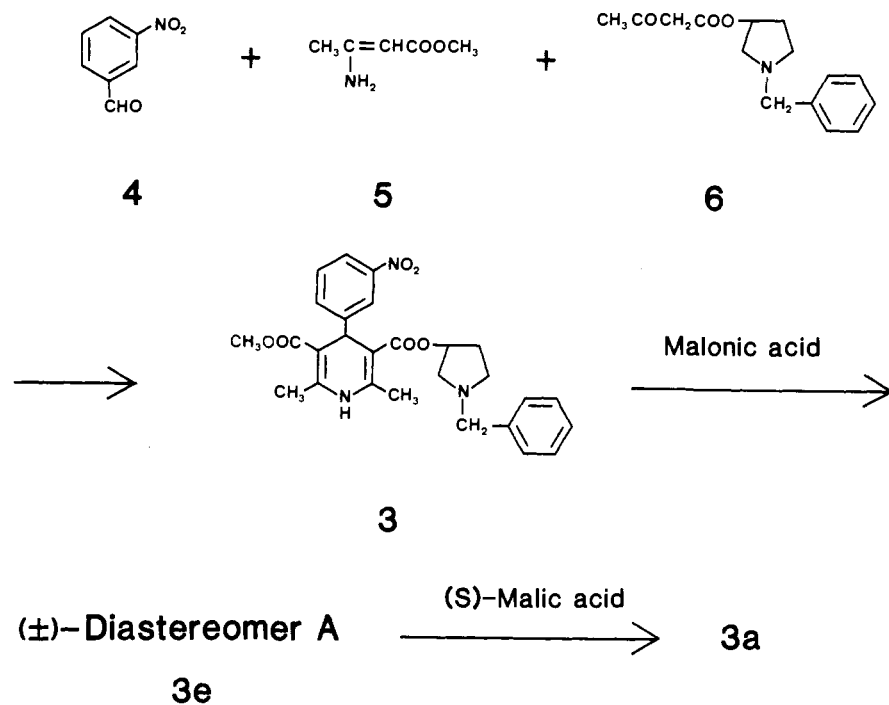
Scheme III
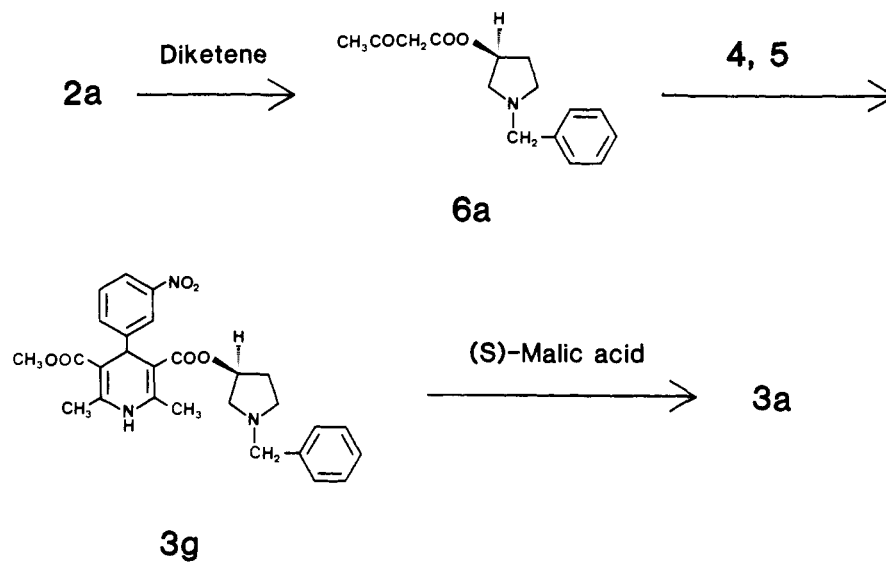
derivatives. Closer examination of **3a·HCl** and **3a·HBr** has indicated that their DHP rings possess the same mode of puckering defined as a set of the signs of the six intraring torsion angles around the bonds of N1–C2, C2–C3, and so on, in spite of their different carbonyl arrangements. The signs of **3a·HCl** and **3a·HBr** are – – + – + +, where, for example, the fourth sign (–) means that the torsional angle around C4–C5 is minus (see crystallographic section). The same puckering mode is also found in the molecular structure of (S)-DHP in the crystals of racemic compounds.[23] This puckering mode may be the essential conformation of (S)-DHP rings. We have assumed that a DHP ring possesses S-chiral character[9b] if the puckering mode is – – + – + +. This enables us to assign the latent chiral character of every molecule that has a nonchiral C4 atom in the DHP ring and is related by mirror or glide

symmetry in the crystal. The chiral characters of the DHP rings according to the assumption and arrangement of the carbonyl groups are summarized in Table III. In DHP derivatives with S character, the carbonyl group at C5 is in the sp arrangement without exception. It should be noted that the sp arrangement of the carbonyl group at C5 is observed in every (S)-DHP derivative regardless of the wide variety of crystal packing as well as of the ester and phenyl substituents. This might suggest that the correlation between S chirality and sp arrangement of the carbonyl group at C5 of the DHP ring is conserved when DHP derivatives bind with DHP receptors.[23b] The structural restriction on the carbonyl group at C5 of the (S)-DHP ring may be favorable for interaction[23b] with DHP receptors and cause the stereoselectivity of antagonism.

Triggle et al.[9b] have studied some nifedipine derivatives with the identical ester groups at C3 and C5 and have reported the linear relationship between the inter-ring conformational angle of ϕ[C3–C4–C7–C8] and distortion

(23) (a) Tacke, R.; Bentlage, A.; Sheldrick, W. S.; Ernst, L.; Towart, R.; Stoepel, K. *Z. Naturforsch., B: Anorg. Chem., Org. Chem.* **1982**, *37B*, 443. (b) Fossheim, R. *J. Med. Chem.* **1986**, *29*, 305.

Table III. Conformations of Carbonyl Groups at C3 and C5 of (S)-1,4-Dihydropyridine Derivatives in Crystal
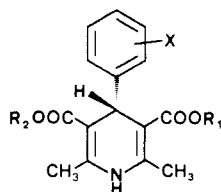
compd	X	R_1	R_2	conformation of carbonyl group[a] C3	C5
3a·HCl	m-NO$_2$	(S)-1-benzyl-3-pyrrolidinyl	CH$_3$	sp	sp
3a·HBr				ap	sp
I[b]	m-NO$_2$	CH$_2$Si(CH$_3$)$_3$	CH$_2$C(CH$_3$)$_3$	sp	sp
II[c]	o,m-Cl$_2$	CH$_2$CH$_3$	CH$_3$	sp	sp
IV[d]	F$_5$	CH$_3$	CH$_3$	sp	sp
V[d]	p-(CH$_3$)$_2$N	CH$_3$	CH$_3$	ap	sp
VI[d]	o-NO$_2$	CH$_3$	CH$_3$	ap	sp
VII[d]	m-CN	CH$_3$	CH$_3$	sp	sp
VIII[d]	H	CH$_3$	CH$_3$	ap	sp
IX[d]	m-NO$_2$	CH$_3$	CH$_3$	ap	sp
X[d]	p-NO$_2$	CH$_3$	CH$_3$	ap	sp
XI[d]	o,p-(NO$_2$)$_2$	CH$_3$	CH$_3$	ap	sp
XII[d]	p-CH$_3$	CH$_3$	CH$_3$	ap	sp
XIII[d]	m-CH$_3$	CH$_3$	CH$_3$	ap	sp
XIV[d]	H	CH$_2$CH$_3$	CH$_2$CH$_3$	ap	sp

[a] ap: antiperiplanar to the C2–C3 or C5–C6 double bond. sp: synperiplanar to the C2–C3 or C5–C6 double bond. [b] Reference 23a. [c] Reference 23b. [d] Reference 9b.

($\Sigma|\tau|$) from planarity of DHP rings for compounds with ortho phenyl hydrogens. Their correlation is based on the molecular structures whose DHP rings are in the $+ + - + - -$ puckering mode. According to our assignment of the latent chiral character, the DHP rings should possess R character. Their correlation should be applied only to (R)-DHP derivatives. In fact, plots of ϕ against $\Sigma|\tau|$ of our (S)-DHP compounds ($\phi = 51$, $\Sigma|\tau| = 74$ for 3a·HCl and $\phi = 88$, $\Sigma|\tau| = 114.3$ for 3a·HBr) do not lie on their regression line. However, the points of ϕ vs. $\Sigma|\tau|$ obtained from (R)-DHP structures generated by inversion of our 3a compounds do lie on their regression line.

Experimental Section

Chemistry. Melting points and boiling points are uncorrected. The structures of the compounds were supported by NMR, IR, and mass spectra. All solid compounds were analyzed (C, H, N, Cl, Br), and values obtained were within ±0.4% of the theoretical values unless otherwise indicated. The organic extracts were dried over MgSO$_4$, and all evaporations were carried out under reduced pressure. Diastereomeric purity of isomers of YM-09730 (3) was determined by HPLC analysis, which was carried out on a 4.6 mm ϕ × 300 mm column packed with Nucleosil 5C$_{18}$ (Marchery Nagel) with a mobile phase of 0.05 mol/L KH$_2$PO$_4$ (pH 3) containing 3 mmol/L tetra-n-pentylammonium bromide as a counterion at a flow rate of 0.9 mL/min. The retention times of diastereomers A and B of 3 were 28 and 29 min, respectively. NMR spectra were recorded on a JEOL FX-100 NMR spectrometer. Optical purity of 2a and 2b was evaluated in the salt with (R)-mandelic acid. NMR spectra of the methylene protons in the benzyl group of 2a (R)-mandelate and 2b (R)-mandelate, respectively, show characteristic signals of a singletlike triplet at 4.03 ppm and a double doublet at 4.01 ppm in CDCl$_3$. The composition of 2a (R)-mandelate was successfully plotted vs. the peak height ratio of Hs/(Hs + Hr), where Hs and Hr were the peak heights at 4.03 ppm of 2a (R)-mandelate and at 3.95 ppm of 2b (R)-mandelate, respectively. Specific rotations were determined with a Perkin-Elmer 241 polarimeter.

(S)-1-**Benzyl-3-hydroxysuccinimide** (7).[13] A mixture of (S)-malic acid (58.2 g, 434 mmol) and benzylamine (48.8 g, 456 mmol) in ethanol (75 mL) was heated. Ethanol and water produced in the reaction were gradually distilled off. The oily residue was heated at 165–170 °C for 2 h. Toluene (160 mL) was added, and the mixture was refluxed for 1 h to remove water produced in the toluene azeotrope. The mixture was allowed to stand at 5 °C overnight. The precipitated crystals were collected by filtration to give 70.7 g (85%) of 7. The product was used in the next step without further purification. Silica gel column chromatography (toluene–ethyl acetate, 2:1, v/v) followed by recrystallization from toluene gave crystals for analysis: mp 99–101 °C; $[\alpha]^{20}_D$ −51.1° (c 1, methanol). Anal. (C$_{11}$H$_{11}$NO$_3$) C, H, N.

(S)-1-**Benzyl-3-pyrrolidinol** (2a).[13] Boron trifluoride etherate (32.1 g, 72.6 mmol) was added dropwise to a cooled solution (0–5 °C) of sodium borohydride (8.2 g, 216 mmol) in anhydrous diglyme (250 mL). The mixture was stirred at 0–5 °C for 30 min followed by dropwise addition of a solution of 7 (22.0 g, 107 mmol) in anhydrous diglyme (65 mL) at the same temperature. The mixture was heated at 100 °C for 15 h with stirring. After cooling, the reaction mixture was concentrated. To the residue obtained was added 6 N HCl (80 mL), and the resulting mixture was heated at 100 °C until evolution of gas had ceased. The mixture was cooled and washed twice with CHCl$_3$ (150 mL). The aqueous layer was alkalized with Na$_2$CO$_3$ (62 g), and the oil that separated was extracted twice with CHCl$_3$ (50 mL). The combined extract was concentrated, and the residue was distilled to afford 13.8 g (73%) of 2a: bp 109–115 °C (0.8 mmHg); $[\alpha]^{20}_D$ −3.0° (c 5, methanol). The optical purity of the alcohol obtained was 80% ee (S) by NMR analysis. The alcohol obtained (12.4 g, 70 mmol) and (R)-mandelic acid (10.64 g, 70 mmol) were dissolved in acetone (46 mL) with heating, and the solution was allowed to stand at 4 °C overnight. The deposited crystals were collected (20.6 g) by filtration and recrystallized twice from acetone (30 mL) to provide 18.1 g (79%) of 2a (R)-mandelate: mp 101–102 °C; $[\alpha]^{20}_D$ −45.5° (c 1, methanol). No R isomer was detected by NMR analysis. The crystals of 2a (R)-mandelate (17.0 g, 51.7 mmol) were dissolved in chloroform (50 mL) and treated twice with a 14% aqueous solution of Na$_2$CO$_3$ (70 mL × 2). The organic layer was concentrated and distilled to afford 8.6 g (94%) of optically pure 2a: bp 115–120 °C (1.2–1.5 mmHg); $[\alpha]^{20}_D$ −3.77° (c 5, methanol).

Resolution of (±)-1-**Benzyl-3-pyrrolidinol** (2). A solution of 2[12] (17.7 g, 100 mmol) and (R)-mandelic acid (15.2 g, 100 mmol) in acetone (66 mL) was allowed to stand at 4 °C overnight. The deposited crystals were collected (8.5 g) by filtration and recrystallized twice from acetone (26 mL) to give 5.1 g (16%) of optically pure crystals of 2a (R)-mandelate. Physical constants of these crystals were in accord with those described above. The crystals were converted to 2a in the same manner.

The prisms precipitated from the mother liquor of the original crystallization were collected by filtration (9.7 g) and recrystallized twice from acetone to afford 5.4 g (17%) of optically pure large prisms of 2b (R)-mandelate: mp 131–132 °C; $[\alpha]^{20}_D$ −48.2° (c 1, methanol). The S-enantiomer 2a was not detected by NMR analysis. Alcohol 2b was regenerated from the mandelate (5.0 g, 15.2 mmol) in the same way as 2a to yield 2.15 g (80%): bp 116 °C (0.9 mmHg); $[\alpha]^{20}_D$ +3.76° (c 5, methanol).

(R)-5-(**Methoxycarbonyl**)-2,6-**dimethyl**-4-(m-**nitrophenyl**)-1,4-**dihydropyridine**-3-**carboxylic acid** (1a): mp 194–195 °C (lit.[2] mp 196–197 °C); $[\alpha]^{20}_D$ −21.2° (c 1, methanol) (lit.[2] $[\alpha]^{20}_D$ −19.6° (c 1, methanol)).

(S)-5-(**Methoxycarbonyl**)-2,6-**dimethyl**-4-(m-**nitrophenyl**)-1,4-**dihydropyridine**-3-**carboxylic acid** (1b): mp 192–194 °C (lit.[2] mp 194–195 °C); $[\alpha]^{20}_D$ +20.9° (c 1, methanol) (lit.[2] $[\alpha]^{20}_D$ +19.1° (c 1, methanol)).

(3S)-1-**Benzyl**-3-**pyrrolidinyl Methyl** (4S)-2,6-**Dimethyl**-4-(m-**nitrophenyl**)-1,4-**dihydropyridine**-3,5-**dicarboxylate** (3a). A suspension of 1a (880 mg, 2.65 mmol) in dimethylformamide (1.2 mL) and dichloromethane (4.8 mL) was cooled at 0–5 °C, and this temperature was maintained during the reaction. Thionyl chloride (0.2 mL, 2.76 mmol) was added dropwise to the suspension, and the mixture was stirred for 1 h. A solution of 2a (490 mg, 2.77 mmol) in dichloromethane (3 mL) was added dropwise to the reaction mixture. After the mixture was stirred for 15 h, it was diluted with dichloromethane (10 mL) and washed with water (10 mL). The organic layer separated was concen-

Table IV. Optical Rotations and Melting Points of the Four Enantiomers of **3**

compound	mp, °C	$[\alpha]^{20}_D$ (c 1, MeOH)
3a·HCl	226–228	+116.4
3a base	137–139	+64.8
3b·HCl	227–230	+56.3
3b base	155–156	−10.3
3c·HCl	228–229	−55.9
3c base	153–155	+10.8
3d·HCl	226–229	−116.5
3d base	136–138	−64.6

Table V. Crystal Data and Details of Experiment and Analysis

	3a·HCl	**3a**·HBr
Crystal Data		
Fw	528.0	572.5
space group	$P2_1$	$P2_12_12_1$
a, Å	14.429 (4)	16.193 (6)
b, Å	7.584 (2)	22.473 (6)
c, Å	12.661 (4)	7.275 (2)
β, deg	93.64 (2)	
V, Å³	1383	2647
Z	2	4
d_{calcd}, g cm⁻³	1.27	1.436
μ(Mo Kα), mm⁻¹	0.188	1.695
Details of Experiment and Analysis		
radiation	Mo	Mo
scan mode	$\omega/2\theta$	$\omega/2\theta$
scan width, deg in ω	1.3 + 0.5 tan θ	0.8 + 0.5 tan θ
scan speed, deg (in ω) min⁻¹	2	2
2θ range, deg	2.0–55.0	2.0–55.0
no. of unique reflections	3414	3450
no. of zero reflections	375	613
q	0.0052	0.011
R	0.12	0.091
no. of reflections for R	2026	1800
maximum shift of parameters	1σ	0.4σ
F_{lim}	0.204	0.384

trated, and the residue was crystallized from methanol to afford 900 mg (64%) of **3a**·HCl. Anal. ($C_{27}H_{30}N_3O_6Cl$) C, H, N, Cl. The melting point and specific rotation are shown in Table IV.

A suspension of **3a**·HCl (800 mg, 1.52 mmol) in chloroform (10 mL) was vigorously shaken with saturated aqueous NaHCO₃ (10 mL × 2) and water (10 mL), successively. The separated organic layer was concentrated, and the residue was crystallized from ethanol to give 640 mg (86%) of free base **3a**. Anal. ($C_{27}H_{29}N_3O_6$) C, H, N.

The hydrobromide of **3a** was obtained by treating a solution of **3a** base (4.92 g, 10 mmol) in chloroform (50 mL) with 1 N HBr (20 mL × 2). After evaporation of the organic layer, the residue was crystallized from methanol to give 5.3 g (93%): mp 238–240 °C dec; $[\alpha]^{20}_D$ +107.6° (c 1, methanol). Anal. ($C_{27}H_{30}N_3O_6Br$) C, H, N, Br.

In a similar manner, hydrochlorides and free bases of **3b**, **3c**, and **3d** were synthesized from **1a** and **2b**, **1b** and **2a**, and **1b** and **2b**, respectively. The melting points and specific rotations of these compounds are shown in Table IV.

(3R*)-1-Benzyl-3-pyrrolidinyl Methyl (4R*)-2,6-Dimethyl-4-(m-nitrophenyl)-1,4-dihydropyridine-3,5-dicarboxylate (3e). Diketene (0.84 g, 10 mmol) was added dropwise to **2** (1.77 g, 10 mmol) at 50–70 °C, and the mixture was heated at 70–80 °C for 1 h to obtain (±)-1-benzyl-3-pyrrolidinyl 3-oxobutyrate (**6**) quantitatively as an oil. A solution of m-nitrobenzaldehyde (**4**, 1.51 g, 10 mmol), methyl 3-aminocrotonate (**5**, 1.15 g, 10 mmol), and **6** (2.61 g, 10 mmol) in 2-propanol (5 mL) was heated under reflux for 8 h. After evaporation of the solvent, (±)-1-benzyl-3-pyrrolidinyl methyl 2,6-dimethyl-4-(m-nitrophenyl)-1,4-dihydropyridine-3,5-dicarboxylate (**3**) was obtained as a caramel (4.91 g). The diastereomeric ratio of the product was ca. 1:1. To a solution of the caramel in acetonitrile (5 mL) was added malonic acid (1.04 g, 10 mmol) in acetonitrile (10 mL), and the resulting solution was allowed to stand at 4 °C overnight. Precipitated crystals were collected by filtration to obtain **3e** malonate (2.03 g). The ratio of the product was 89.1:10.9. The product was recrystallized twice from 25 vol of methanol to provide 1.0 g (17%) of **3e** malonate, which showed a single peak at 28 min by HPLC: mp 181.5–182.5 °C dec. Anal. ($C_{30}H_{31}N_3O_{10}$) C, H, N.

A suspension of **3a** malonate (1.0 g, 1.68 mmol) in chloroform (10 mL) was treated with saturated aqueous NaHCO₃ (10 mL × 2) and water (10 mL), successively. The solvent was removed, and the residue was crystallized from ethanol (1.6 mL) to give 0.75 g (91%) of **3e**: mp 145–148 °C. Anal. ($C_{27}H_{29}N_3O_6$) C, H, N.

Resolution of 3e. (S)-Malic acid (1.34 g, 10 mmol) and **3e** (4.91 g, 10 mmol) were dissolved in ethanol (30 mL) with heating, and the solution was allowed to stand for 2 days at 4 °C. Deposited crystals were collected by filtration and recrystallized from methanol (35 mL) to obtain 2.6 g (42%) of **3a** (S)-malate: mp 190–191 °C dec; $[\alpha]^{20}_D$ +82.2° (c 0.5, methanol). No change of the specific rotation was observed with additional recrystallizations. Anal. ($C_{31}H_{35}N_3O_{11}$) C, H, N. The malate (2.5 g, 4.0 mmol) in chloroform (50 mL) was treated successively with saturated NaHCO₃ (20 mL × 2), water (20 mL), and 1 N HCl (20 mL × 2). The organic layer separated was evaporated, and the residue was crystallized from methanol to give 1.8 g (85%) of **3a**·HCl: mp 228–230 °C dec; $[\alpha]^{20}_D$ +116.2° (c 1, methanol). Anal. ($C_{27}H_{30}N_3O_6Cl$) C, H, N, Cl.

(3S)-1-Benzyl-3-pyrrolidinyl Methyl (4R/S)-2,6-Dimethyl-4-(m-nitrophenyl)-1,4-dihydropyridine-3,5-dicarboxylate (3g). To an oily product **6a** (2.61 g, 10 mmol)

obtained by the reaction of diketene (0.84 g, 10 mmol) and **2a** (1.77 g, 10 mmol) in the same manner as **6** were added **4** (1.51 g, 10 mmol), **5** (1.15 g, 10 mmol), and 2-propanol (5 mL). The mixture was heated under reflux for 8 h and evaporated to give crude caramel of **3g** base (4.91 g). The product was a diastereomeric mixture of **3a** and **3c** (ca. 1:1). The caramel obtained and oxalic acid dihydrate (1.26 g, 10 mmol) were dissolved in a mixture of acetone (15 mL) and toluene (15 mL) with heating and allowed to stand at 4 °C overnight to obtain 4.61 g (78%) of crystals of **3g** oxalate: mp 113–115 °C. Anal. ($C_{29}H_{31}N_3$-O_8·0.5H₂O) C, H, N. The diastereomeric ratio of the oxalate was ca. 1:1. From the oxalate, 3.82 g (77% based on **2a**) of **3g** base was regenerated as a caramel in a usual manner.

Selective Crystallization of 3a from 3g. The purified **3g** base (2.46 g, 5 mmol) and (S)-malic acid (0.67 g, 5 mmol) were dissolved in acetone (12 mL) and allowed to stand at 4 °C for 3 days to give crystals of **3a** (S)-malate (1.18 g), which were recrystallized twice from methanol to yield 810 mg (26%): mp 190–191 °C; $[\alpha]^{20}_D$ +82.8° (c 0.5, methanol). The hydrochloride of **3a** (710 mg, 84% yield) was obtained from the malate (1.0 g, 1.6 mmol) in a usual manner. The melting point and specific rotation were identical with those of **3a**·HCl obtained in the preceding paragraph. Anal. ($C_{27}H_{30}N_3O_6Cl$) C, H, N, Cl.

Binding Assays. Male Wistar rats (7–9 weeks old) were killed by decapitation. The cerebral cortex was quickly removed, chilled in ice-cold 0.85% NaCl, and homogenized in a motor-driven Teflon homogenizer with 9 vol of 50 mmol/L Tris·HCl buffer and 10 mmol/L EDTA, pH 7.7, and the homogenates were centrifuged at 900g for 10 min. The supernatant fluids were further centrifuged at 18000g for 20 min, the pellets were washed twice with 50 mmol/L Tris·HCl, 0.1 mmol/L EDTA, pH 7.7, and the resulting pellets were suspended in the same buffer and stored at −80 °C. [³H]Nitrendipine binding was determined by the method of Gould et al.[16] as follows: Triplicate polystyrene tubes contained various concentrations of the calcium antagonist, 0.5 pmol of [³H]nitrendipine (173.2 dpm/fmol, New England Nuclear), 50 μmol of Tris·HCl, 0.1 μmol of EDTA, 1 μmol of CaCl₂, pH 7.7, and 0.4 mg of protein of membrane preparations (K_d and B_{max} values for [³H]nitrendipine of the preparations were about 0.4 nmol/L and 150 fmol/mg, respectively) in the final volume of 1 mL. Incubations were performed at 25 °C for 60 min in the dark, and the mixtures were rapidly filtered under vacuum through Whatman GF/B filters. Then filter disks were washed four times with 4 mL each of 50 mmol/L Tris·HCl and 0.1 mmol/L EDTA, pH 7.7, and dried at 70 °C for about 60 min. The radioactivity was counted in 10 mL of Bray–dioxane scintillator in a Packard liquid scintillation counter lined to a HP-85 computer (Hewlett-Packard). Calcium antagonists were dissolved in 90%

Table VI. Fractional Coordinates and Isotropic Temperature Factors of 3a·HCl and 3a·HBr[a]

Atom	x	y	z	$B/Å^2$	Atom	x	y	z	$B/Å^2$
CL	0.4570(3)	0.49249	-0.1060(3)	4.2<20>	BR	0.49601(6)	0.01025(3)	0.71964(9)	4.60<116>
N1	0.3459(8)	0.421(2)	0.6658(8)	3.3<13>	N1	0.3890(3)	0.2722(2)	0.7696(7)	2.9<7>
C2	0.399(1)	0.419(2)	0.580(1)	3.2<7>	C2	0.4119(4)	0.2285(3)	0.6443(9)	2.4<7>
C3	0.3569(9)	0.399(2)	0.4787(9)	2.0<11>	C3	0.3794(4)	0.2294(3)	0.4744(9)	2.3<10>
C4	0.2547(9)	0.356(2)	0.461(1)	2.1<10>	C4	0.3111(4)	0.2728(3)	0.4271(9)	2.6<9>
C5	0.2058(9)	0.408(2)	0.5628(9)	2.2<8>	C5	0.3204(4)	0.3295(3)	0.5436(9)	2.2<6>
C6	0.2487(9)	0.432(2)	0.662(1)	3.7<21>	C6	0.3531(4)	0.3262(3)	0.7123(9)	2.4<11>
C21	0.5038(9)	0.442(2)	0.605(1)	3.3<13>	C21	0.4705(4)	0.1848(3)	0.7317(9)	2.8<17>
C31	0.408(1)	0.406(2)	0.379(1)	3.7<27>	C31	0.4053(4)	0.1909(2)	0.3251(8)	1.9<8>
O32	0.4932(6)	0.440(2)	0.3789(7)	4.2<20>	O32	0.3750(3)	0.1890(2)	0.1750(6)	3.7<28>
O33	0.3547(6)	0.373(2)	0.2909(7)	3.2<10>	O33	0.4743(3)	0.1571(2)	0.3634(6)	3.0<9>
C34	0.399(1)	0.379(2)	0.190(1)	3.3<26>	C34	0.5040(5)	0.1179(2)	0.2203(8)	2.8<11>
C35	0.418(1)	0.575(2)	0.165(1)	3.4<7>	C35	0.4477(4)	0.0638(3)	0.200(1)	3.3<16>
N36	0.3488(8)	0.622(2)	0.0759(8)	3.0<17>	N36	0.4998(3)	0.0138(2)	0.2778(7)	3.5<13>
C37	0.274(1)	0.488(3)	0.076(1)	3.9<22>	C37	0.5888(3)	0.0290(3)	0.2470(9)	2.8<13>
C38	0.325(1)	0.321(3)	0.108(1)	4.2<36>	C38	0.5904(4)	0.0967(3)	0.284(1)	3.4<12>
C39	0.317(1)	0.807(2)	0.079(1)	3.2<11>	C39	0.4765(4)	-0.0479(3)	0.215(1)	3.9<10>
C40	0.273(1)	0.868(2)	-0.024(1)	3.7<12>	C40	0.3849(4)	-0.0611(2)	0.235(1)	3.4<21>
C41	0.330(1)	0.914(3)	-0.098(1)	5.4<25>	C41	0.3564(5)	-0.0794(3)	0.408(1)	4.0<15>
C42	0.299(1)	0.972(3)	-0.194(1)	6.4<29>	C42	0.2750(5)	-0.0923(4)	0.428(2)	7.0<47>
C43	0.202(1)	1.002(3)	-0.210(1)	7.0<49>	C43	0.2202(5)	-0.0858(4)	0.287(2)	8.0<57>
C44	0.147(1)	0.955(4)	-0.131(1)	7.5<35>	C44	0.2486(5)	-0.0696(4)	0.115(2)	8.3<44>
C45	0.178(1)	0.888(3)	-0.041(1)	6.2<33>	C45	0.3317(5)	-0.0543(3)	0.091(1)	5.5<20>
C7	0.232(1)	0.163(2)	0.427(1)	3.3<26>	C7	0.2268(4)	0.2447(3)	0.4512(8)	2.0<9>
C8	0.2748(9)	0.022(3)	0.490(1)	3.4<23>	C8	0.1854(4)	0.2456(3)	0.6162(9)	2.0<3>
C9	0.251(1)	-0.154(2)	0.456(1)	4.9<38>	C9	0.1103(4)	0.2180(3)	0.6301(9)	2.9<20>
C10	0.187(1)	-0.169(3)	0.366(1)	7.3<87>	C10	0.0706(4)	0.1893(3)	0.484(1)	3.5<10>
C11	0.144(1)	-0.049(3)	0.298(2)	9.8<111>	C11	0.1115(4)	0.1872(3)	0.325(1)	3.9<22>
C12	0.172(1)	0.121(3)	0.341(1)	3.6<16>	C12	0.1910(4)	0.2155(3)	0.301(1)	3.0<7>
N111	0.0829(9)	-0.076(3)	0.218(1)	8.9<107>	N91	0.0647(3)	0.2235(2)	0.8088(8)	3.8<17>
O112	0.055(1)	0.042(3)	0.170(1)	12.5<52>	O92	0.0936(3)	0.2546(2)	0.9258(7)	4.9<18>
O113	0.078(1)	-0.246(2)	0.204(1)	8.8<52>	O93	0.0021(3)	0.1947(2)	0.8296(7)	5.4<23>
C51	0.103(1)	0.425(2)	0.551(1)	3.9<11>	C51	0.2834(4)	0.3850(3)	0.469(1)	3.5<15>
O52	0.0508(7)	0.435(3)	0.6193(8)	7.7<59>	O52	0.2816(3)	0.4321(2)	0.5420(8)	6.3<40>
O53	0.0741(6)	0.430(2)	0.4461(7)	4.7<27>	O53	0.2505(3)	0.3761(2)	0.3039(7)	4.8<25>
C54	-0.0230(9)	0.436(3)	0.417(1)	5.7<37>	C54	0.2089(5)	0.4267(3)	0.227(1)	5.9<21>
C61	0.211(1)	0.479(3)	0.766(1)	4.7<27>	C61	0.3582(5)	0.3750(3)	0.850(1)	4.0<18>

[a] The B values are the equivalent isotropic temperature factors calculated from anisotropic thermal parameters using the equation $B = 8\pi^2(U_1 + U_2 + U_3)/3$, where U_1, U_2, and U_3 are principal components of the mean square displacement matrix U. Values in ⟨ ⟩ are anisotropicity defined by $(\sum(B - 8\pi^2 U_i)^2/3)^{1/2}$ and those in () are ESD's; they refer to last decimial places.

methanol, 0.1 N HCl at the concentration of 20 mmol/L and diluted with 10% methanol, and the final methanol concentration in the reaction mixture was kept below 0.5%. Specific binding was defined as the excess over blank in the presence of 10 μmol/L (±)-nicardipine. The K_i values were computed from the IC$_{50}$ values, the concentrations required to inhibit specific binding by 50%, from the linear regression of logit-log method.[24,25]

Determination of Coronary Blood Flow. Adult mongrel dogs of either sex weighing from 8 to 15 kg were used. Anesthesia was induced by a single intravenous injection of pentobarbital sodium (30 mg/kg) and maintained by intravenous infusion of the same anesthetic at a rate of 3-5 mg kg^{-1} h^{-1}. The trachea was intubated, and the animals were ventilated artificially with room air in a tidal volume of 20 mL/kg at 18-20 breaths/min with use of a respirator (Harvard Apparatus or Shinano Seisakusho, Tokyo, Japan). A thoracotomy was performed at the fourth intercostal space. After an intravenous injection of heparin (1000 units/kg),

arterial blood from the distal end of the cannula to the left common carotid artery was led to the circumflux branch of the left coronary artery by an extracorporeal loop. A servocontrolled pump (Model 1251D, Harvard Apparatus) was incorporated in the circuit to maintain a constant perfusion pressure of 120 mmHg by means of a pump controller (SCS-22, Data Graph Co., Tokyo, Japan). An electromagnetic flow probe of extracorporeal type (Nihon Kohden, Tokyo, Japan) was inserted in the circuit to record coronary blood flow (CBF). Arterial blood pressure was measured with a pressure transducer (MPU-0.5, Nihon Kohden) connected to a catheter inserted into the femoral artery, and heart rate was measured by a cardiotachometer (AT-600G, Nihon Kohden) triggered by the pulse wave of the arterial pressure. All recordings were made on a Nihon Kohden multichannel recorder (RM-600). In this method, vasodilation increases blood flow independently of systemic blood pressure. Basal coronary blood flow was 27.1 ± 0.7 mL/min in 20 anesthetized dogs. The drug solutions were administered directly into the rubber tubing connected close to the coronary artery cannula in a volume of 0.1 mL for a period of 10 s. Three to four doses of one isomer were evaluated in a single dog and given in increasing order after CBF returned to base-line or near-base-line levels.

Crystallographic Work. Crystals of 3a·HCl and 3a·HBr suitable for X-ray diffraction studies were grown from methanol.

(24) Terai, M.; Takenaka, T.; Maeno, H. *Methods in Biogenic Amine Research*; Elsevier: Amsterdam, The Netherlands, 1983; p 573.

(25) De Lean, A.; Munson, P. J.; Rodbard, D. *Am. J. Physiol.* **1978**, *235*, E97.

Measurements of diffraction were carried out on a Rigaku AFC-5R diffractometer, using graphite-monochromated Mo Kα radiation (λ = 0.710 73 Å). The unit cell dimensions were obtained by least squares of 20 2θ values.

Five reference reflections monitored showed no significant intensity deterioration during data collection. Corrections were made for Lorentz and polarization factors but not for absorption. Weak reflections below background were regarded as zero reflections. The standard deviations were estimated by the equation $\sigma^2(F_o) = \sigma_p^2(F_o) + q^2F_o^2$, where q was derived from measurement of the monitored reflections and $\sigma_p(F_o)$ was due to counting statistics.[26] The crystal data and experimental details are summarized in Table V. The structure of 3a·HBr was solved by a combination of heavy-atom and direct-method techniques.[27] The Br coordinates were derived from a Patterson synthesis. After least-squares refinement of the coordinates, weighted Fourier method revealed the remaining non-H atoms. The structure of 3a·HCl was solved by the direct method. The atomic parameters were refined by the blocked-diagonal least-squares method. The quantity minimized was $\Sigma\omega(|F_o| - |F_c|)^2$ with $\omega = 1/\sigma^2(F_o)$. In the refinement, the zero reflections with $|F_c| > F_{lim}$ were included by assuming $|F_o| = F_{lim}$ with $\omega = \omega(F_{lim})$, F_{lim} being the observed threshold value. The hydrogen atoms were obtained by calculation and fixed. In the last cycle of refinement, H atoms were included in the calculation of structure factors and the R values were 0.12 for 3a·HCl with 1.0σ of the maximum shift in the atomic parameters and 0.091 for 3a·HBr with 0.4σ. The final atomic parameters of 3a·HCl and 3a·HBr are given in Tables VIa and VIb, respectively.

The absolute configuration of 3a·HBr has been determined by the Bijvoet method from the anomalous scattering due to the Br atom with use of Mo radiation and found to be S,S.

The atomic scattering factors were taken from *International Tables for X-ray Crystallography*.[28]

(26) McCandlish, L. E.; Shout, G. H.; Andrews, L. C. *Acta Crystallogr., Sect. A: Cryst. Phys., Diffr., Theor. Gen. Crystallogr.* 1975, *A31*, 245.

(27) Main, P.; Hull, S. E.; Lessinger, L.; Germain, G.; Declercq, J. P.; Woolfson, M. M. *Multam 78. A System of Computer Programs for the Automatic Solution of Crystal Structures from X-ray Diffraction Data*; University of York, York, England, 1978.

(28) *International Tables for X-ray Crystallography*; Kynoch: Birmingham, England, 1974; Vol. 4.

Substituted-Vinyl Hydroxytriarylethylenes, 1-[4-[2-(Diethylamino)ethoxy]phenyl]-1-(4-hydroxyphenyl)-2-phenylethylenes: Synthesis and Effects on MCF 7 Breast Cancer Cell Proliferation

Peter C. Ruenitz,*[,†] Jerome R. Bagley,[†] Colin K. W. Watts,[‡] Rosemary E. Hall,[‡] and Robert L. Sutherland[‡]

College of Pharmacy, University of Georgia, Athens, Georgia 30602, and Garvan Institute of Medical Research, St. Vincent's Hospital, Sydney, N.S.W. 2010, Australia. Received March 6, 1986

A series of triarylethylene compounds related to 4-hydroxyclomiphene (2) in which the vinyl Cl substituent was replaced by ethyl (5), Br (6), H (7), CN (8), or NO$_2$ (9) substituents were synthesized to facilitate studies of the molecular actions of synthetic nonsteroidal antiestrogens. The relative binding affinities of these compounds for the estrogen receptor (ER) and the antiestrogen binding site (AEBS) in MCF 7 human mammary carcinoma cells were measured and correlated with the effects of these drugs on cell proliferation kinetics. Affinities for ER and AEBS were highly correlated, illustrating that vinyl substituents influence binding to ER and AEBS in a parallel manner. All compounds except 7 had biphasic effects on cell proliferation kinetics, indicating the presence of at least two distinct mechanisms by which hydroxytriarylethylenes inhibit breast cancer cell proliferation. In the concentration range 10^{-10}–10^{-8} M, cell proliferation was inhibited by 60–70%, these effects were estrogen-reversible, and the degree of growth inhibition was in the order Cl > Et > Br > NO$_2$ > CN > H, which paralleled the order of affinities for ER. There was no further inhibition of cell growth between 10^{-8} and 10^{-6} M, but at concentrations >10^{-6} M there was a further dose-dependent decrease in cell growth mediated by mechanisms yet to be defined but apparently distinct from ER-mediated events. In both concentration ranges, growth inhibition was accompanied by accumulation of cells in the G$_1$ phase of the cell cycle. These data, obtained with a novel series of hydroxytriarylethylenes, have enabled clear definition of two distinct mechanisms of growth inhibition by triarylethylene antiestrogens. They also indicate that among the vinyl substitutions examined to date the Cl substituent yields the most active molecule both in terms of affinity for ER and AEBS and potency as a growth inhibitory agent.

Triarylethylene antiestrogens such as tamoxifen (1)[1] are of considerable interest due primarily to their ability to antagonize the growth of some hormone-dependent tumors, particularly breast cancer.[2] Although the mecha-

---

† University of Georgia.

‡ St. Vincent's Hospital.

(1) For convenience, the "trans" configurations of 1 and other triarylethylenes are illustrated.